NATIONAL ADVISORY COMMITTEE FOR AERONAUTICS

TECHNICAL NOTE 3856

FATIGUE-CRACK PROPAGATION IN ALUMINUM-ALLOY BOX BEAMS

By Herbert F. Hardrath, Herbert A. Leybold, Charles B. Landers, and Louis W. Hauschild

Langley Aeronautical Laboratory
Langley Field, Va.

Washington
August 1956

NATIONAL ADVISORY COMMITTEE FOR AERONAUTICS

TECHNICAL NOTE 3856

FATIGUE-CRACK PROPAGATION IN ALUMINUM-ALLOY BOX BEAMS

By Herbert F. Hardrath, Herbert A. Leybold, Charles B. Landers, and Louis W. Hauschild

SUMMARY

Eighteen box beams constructed according to four designs were subjected to fatigue tests to study fatigue-crack propagation and accompanying stress redistribution. Two designs had stiffeners riveted to the cover, one had stiffeners bonded to the cover, and one had an integrally stiffened cover machined from a plate. Two or more specimens of each design were constructed from each of the aluminum alloys 2024-T3 and 7075-T6. The rate of crack propagation in specimens made of 7075-T6 material was more rapid than that in equivalent specimens made of 2024-T3 and tested at the same nominal stress. Specimens with bonded stringers had lower rates of crack growth than did other specimens. The most rapid rate of crack propagation was found in specimens having covers that were integrally stiffened. The results are discussed with the aid of stress-survey data obtained during the tests.

INTRODUCTION

The occurrence of several catastrophic or nearly catastrophic accidents caused by fatigue cracks in the primary structure of airplanes has prompted considerable discussion regarding "fail-safe" design philosophy. Proponents of this philosophy recommend that aircraft structures be constructed in such a way that fatigue cracks which might occur do not cause catastrophic failure before remedial action can be taken.

From the designer's point of view, several important questions must be answered before a structure may be called fail-safe. Among these are the following:

(1) Where is crack initiation most likely to occur?

(2) Will a crack propagate in such a way that it is likely to be discovered before it is dangerously large?

(3) What can be done to control crack propagation?

(4) What is the residual static strength of the structure after a crack forms?

The National Advisory Committee for Aeronautics is currently studying several phases of this general problem. The present paper presents initial results of tests intended to provide information concerning questions (2) and (3). Four designs of box beams were built according to current construction techniques, from both 2024-T3 and 7075-T6 aluminum alloy, and were subjected to constant-level fatigue tests at the same nominal stress. Fatigue-crack propagation was observed and strain-gage surveys were made at various stages of the tests in order to study the redistribution of stress resulting from crack growth.

APPARATUS AND TESTS

Specimens

Details of the construction of the four different designs of beams tested are shown in figures 1 to 4. At least two specimens of each design were constructed of each of the aluminum alloys 7075-T6 and 2024-T3. Brazier-head rivets made of 2117-T3 aluminum alloy were used throughout.

Each beam was 8 feet long between supports with a constant-moment section (carry-through bay) 2 feet long in the center. The tension covers of the beams were cambered to compensate for shear lag effects. Bulkheads were placed at 8-inch intervals in the carry-through bay and at 12-inch intervals in the outboard bays. Upright angles were attached to the shear webs at intermediate stations. The compression covers were designed to insure that the tension cover was critical for static loading. All boxes were 20 inches wide and had 8 longitudinal stringers in each cover except design 1, which was 12 inches wide and had 4 longitudinal stringers in each cover. A stress-raiser was placed at or near the center of the tension cover to encourage crack initiation at that point. This section is referred to as the critical section. Two 1/4-inch holes, one on each side of the longitudinal axis, were drilled and reamed so that they were tangent at the center line. The material between the tangents to the two holes was removed with a small file to make an oblong hole, 1/2 inch long and 1/4 inch wide. A hole 1 inch in diameter was drilled in each shear web near the critical section to permit inspection of the stringers during the tests.

The distinguishing features of the various configurations were as follows:

Design 1: Beams built according to design 1 (fig. 1) were 12 inches wide and had four 1/16-inch by 1 inch by 1 inch stringers riveted to a cover made of 0.051-inch sheet. The rivet pitch was 3/4 inch in all stringers and flanges.

Design 2: Beams built according to design 2 (fig. 2) were similar to design 1 except that they were 20 inches wide, had 8 stiffeners, and the rivet pitch in the stringers was $1\frac{1}{2}$ inches.

Design 3: Beams built according to design 3 (fig. 3) were dimensionally identical to design 2 but the stringers were bonded to the tension cover with an ethoxyline resin adhesive. Rivets were omitted in the carry-through bay but were used, in addition to the bonding, in the outboard bays of the cover.

Design 4: Beams built according to design 4 (fig. 4) had integrally stiffened covers machined from a 3/4-inch by 20-inch by $100\frac{3}{8}$-inch plate. The thickness of the skin between stiffeners was 0.081 inch and the stiffener thickness was 0.094 inch. Only the carry-through bay was machined to the dimensions indicated. The two bays at each end of the cover were not machined except for the flanges. A taper in the bays immediately adjacent to the carry-through bay joined the machined and unmachined parts. The cover was not cambered in this type of construction.

For identification, each specimen was given a code designation (for example, 1B-2) to facilitate reference to specific beams. This designation is explained as follows: The first digit is a number corresponding to the design number just described, the letter following this number is used to identify the aluminum alloy from which the beam was built (A is for 2024-T3 and B, for 7075-T6), and the last digit is a number designating the first, second, or third specimen of a given design and material. In the example, specimen 1B-2 represents the second beam constructed of 7075-T6 aluminum alloy according to design 1.

Equipment

The specimens were subjected to repeated loads in a fatigue-testing machine located in the Langley structures research laboratory. A photograph of this machine with a specimen in place is shown in figure 5. The specimens are supported by flexure struts at each outboard corner and loaded through similar struts that attach the four corners of the carry-through bay to a movable crosshead. Forces are controlled by adjustments of a variable-throw crank and adjustable connecting rod. The machine has a load capacity of 20,000 pounds, a maximum eccentricity of 1/2 inch, and operates at approximately 600 rpm.

Instrumentation

Resistance wire strain gages attached to the flexure struts of the testing machine are read individually to check for uniform distribution of loads among the struts. The sum of the outputs of the gages on the four struts on the crosshead is read to monitor the applied load during progress of the test. The electronic apparatus described in reference 1 was used for these readings.

Other resistance wire strain gages were applied to the specimens to check stress distributions in the tension cover during the tests. One gage was placed on the outstanding leg of each stringer at the critical section of the beam. Gages were also applied to the cover of the beam at 1-inch intervals across the width. In the tests of all beams of designs 1 and 2 and of specimen 3B-1 these gages were displaced from the critical section by $1\frac{1}{2}$ inches to permit installation of fatigue-crack detector wires at the critical section. In the remainder of the tests the detector wires were not used and strain gages on the cover were applied at the critical section.

Procedure

In the tests of beams of design 1, several stress levels were used to arrive at a test condition with a mean stress representative of 1 g stresses used in practice and an alternating stress producing failure in a reasonable time. As indicated in figure 6, beam 1A-1 was tested at a stress of 16 ± 6 ksi; beam 1A-2 was tested at a stress of 12 ± 4.6 ksi for 557,000 cycles without initiating a crack and then was tested at a stress of 12 ± 6 ksi. Tests of all other beams of design 1 were performed at a stress of 12 ± 6 ksi. Tests of other designs were performed at stresses of 13 ± 6.5 ksi.

Initial loads in each test were adjusted to produce the desired readings in the strain gages on the specimen. The loads were adjusted as required during the tests to maintain load readings (strain gages on struts) within ±3 percent of the initial readings.

The critical section of the cover was marked at 1/4-inch intervals and the number of cycles of load which had been applied when the fatigue crack passed each of these stations was recorded. In some cases a red dye was used to improve visibility of the crack. Strain-gage readings were taken whenever the crack passed completely through one of the skin panels or stringers. Tests were usually continued until at least one stringer had failed.

RESULTS AND DISCUSSION

Crack Initiation

The number of cycles of load applied to each beam to produce a crack visible to the naked eye is indicated by the shaded parts of the bar graph in figure 6.

Because of the various stress levels used in tests of beams with design 1, the results of those tests are not directly comparable with the results for other designs. The smallest number of cycles of load required to initiate a crack in a beam of design 1 was found in specimen 1A-1, which was also subjected to the highest stress. The largest number of cycles was found in specimen 1A-2, which had been subjected to lower stresses in the first part of the test. Some "coaxing" may have occurred at the lower stress level to cause this long life.

Specimen 4B-1 survived approximately 179,500 cycles of load without a crack developing at the critical section. However, at this time, a loud report was heard and a crack 4 inches long was found in the cover at the support station 12 inches from the critical section. This crack was patched by use of a fiber-glass technique described in reference 2. A similar patch was placed on the station 12 inches to the other side of the critical section and the test resumed. When a total of 226,900 cycles had been applied, another loud report was heard and a crack $6\frac{1}{2}$ inches long was found at a cross section 3 inches from the critical section. This crack had evidently started at a rivet in the corner flange and progressed past two stringers before it was detected. (The region where this crack occurred had been covered with a clamping device which held the leads for strain gages on the box.) The test was discontinued at this point.

Specimen 4B-2 was reinforced with fiber-glass patches at the stations 12 inches to each side of the critical section prior to test. In addition, the effectiveness of the stress-raiser at the center of the beam was increased by making small notches at the ends of the major axis of the hole. Those notches were made by use of a fine thread coated with valve-grinding compound. The notch had a radius of approximately 0.003 inch and was approximately 0.017 inch deep. As expected, the higher stress concentration caused crack initiation earlier in this test than in any other.

The remaining beams, regardless of design, were tested at the same stress level without other complications. The data for these beams should, therefore, be directly comparable to each other. The scatter in number of cycles required to initiate cracks in these beams appears

to be about as would be expected for simple specimens made of the same materials. No significant differences were found between the numbers of cycles of load required to initiate cracks in beams made of 2024-T3 aluminum alloy and those required to initiate cracks in beams made of 7075-T6 aluminum alloy.

For comparison, the fatigue life was predicted for simple specimens containing similar stress-raisers and subjected to the same stresses. This prediction was made as follows: The theoretical stress-concentration factor for the hole at the critical section of each of the beams was estimated by the theory of reference 3 to be 3.8 and the corresponding Neuber technical factor K_N (ref. 4) was 3. This factor, together with average fatigue properties of unnotched sheet specimens published in reference 1, was used to predict a life of 140,000 cycles for complete failure in simple specimens made from either 2024-T3 or 7075-T6 aluminum alloy. Final failure in built-up structures is dependent upon the complexity of the specimen and, therefore, is not readily comparable to failure in simple specimens. The number of cycles required to cause failure of 20 percent of the tension cross section was arbitrarily plotted in figure 6 for comparison. For purposes of this presentation the tension cross section was defined as the net area of that part of the cross section which was above the neutral axis. The neutral axis was computed for the gross section. Reasonable agreement between these values and the predicted life of simple specimens was found.

Crack Propagation

The crack-propagation histories for each of the beams are presented in figures 7 to 10 as curves of the percentage of tension cross-sectional area lost plotted against the number of cycles of load applied after crack initiation. All the curves except those for design 1 are plotted to the same scale to aid in making comparisons.

In general, the cracks started at both sides of the stress-raiser and grew slowly in both directions until at least one panel had failed. The rate of crack growth then increased gradually during the test and, after stiffeners began to fail, became very rapid. The failure of stiffeners was almost always sudden with very little crack propagation visible before complete failure of the stiffener.

Design 1.- The most rapid crack growth for specimens of design 1 was found in beam 1A-1 (fig. 7). This result was expected since the highest stress was used in this test. The crack-propagation curve for beam 1A-2 was essentially the same as that for beam 1A-3, even though 1A-2 had been subjected to 10 times as many cycles of load (including cycles at a lower stress level) before the crack started. The initial part of these curves is concave upward and ends abruptly at a point where

approximately 8 percent of the tension material has failed. This part of the curve represents growth of the crack across the middle panel to the rivet holes in stringers adjacent to the center of the beam. (The term "panel" refers to that part of the cover bounded by stringers.) The crack was then dormant for some time before it started again on the other side of the rivet. The next part of the curve is again concave upward and represents crack growth across the panels adjacent to the middle panel. The cracks usually grew completely through these panels before the middle stiffeners failed. The sudden upward trend of the curve represents failure of the middle stiffeners. The failure of the remaining two panels and two stiffeners followed almost immediately and the test was stopped when the crack reached the rivets in the corner flange. Because of the rapid failure of the beam after loss of the first stringers a decision was made to make the second design with more stringers so that each contributed a smaller percentage of the total tension material.

The crack-propagation curves for the 7075-T6 beams made according to design 1 are similar to those of the 2024-T3 beams, but the number of cycles of load required to produce a given crack length is less in the 7075-T6 beams. In specimen 1B-1 the crack proceeded across the beam along a practically straight line and passed midway between rivets in the first stiffener on one side. Therefore, the crack continued to grow uninterrupted until it reached a rivet hole 3/4 inch away from the critical section in the second stringer on that side. Thus, the abrupt discontinuity in the crack-propagation curve occurs when approximately 14 percent of the material has failed. The rest of the propagation of this crack was essentially the same as for specimen 1B-2 and for 2024-T3 specimens described earlier.

Design 2.- Crack propagation in beams of design 2 (fig. 8) progressed in a manner similar to that in design 1. Generally the skin failed in three panels before the first two stiffeners failed. The rate of propagation in 2024-T3 beams was slightly greater in design 2 than in design 1, probably because of the higher stress level used in the wider beams. Cracks propagated much more rapidly in the 7075-T6 beams in this series than in the 2024-T3 beams. In specimen 2B-1 the crack followed an essentially straight line which missed rivet holes at the first 3 stiffeners on one side of the beam. Consequently, the crack propagation was more rapid in this specimen than in any other of this design. This test was stopped before any stiffeners failed.

Design 3.- In general, in specimens with bonded stringers (design 3), the crack propagated completely across the skin without failure of any stringers. The percentage area lost for a given number of cycles of load (fig. 9) was lower in these specimens than in specimens made of the same material in other designs. One exception to this trend occurred in specimen 3A-1, in which crack propagation was very rapid compared with that in beams 3A-2 and 3A-3. Inspection of beam 3A-1 after failure

revealed that a poor bond existed between the stiffeners and the cover. After the crack had passed the first stiffener, the bonding apparently had little effect and the crack progressed much as though no connections between skin and stiffeners had been present.

Inspection of the bonds in other beams revealed that in no case was the bonding 100 percent effective. Therefore, the results may not be entirely typical for this type of construction. In general, however, the beams which had the better bonds between skin and stiffeners also had the better crack-propagation characteristics. In this respect, the bonds in 7075-T6 beams looked somewhat better than those in the 2024-T3 beams. This may explain why the crack-propagation curves for specimens 3B-1 and 3B-2 compared so favorably with the curve for 3A-3.

The progress of the fatigue crack across the stiffener caused the bond between the skin and stiffener to separate slowly in each direction along the stringer. A light metal object was gently tapped against the skin during the test in order to get an estimate of how far the bond had separated. Inspection of the specimens after tests indicated that this method had been fairly reliable. Figure 11 is a sketch showing the contour of bond separation for various stages of crack growth in specimen 3B-1.

Design 4.- The specimens with machined covers had the most rapid crack growth (fig. 10) of any of the specimens tested. In general, the cracks grew through the middle panel in much the same manner as in other configurations. The first stiffener on each side tended to slow the crack only very slightly. The crack then grew past the stiffener in the skin and down into the stiffener itself. Sudden failure of the stiffener occurred when the crack had penetrated approximately one-half the depth of the stiffener. Usually the next panel also failed before the machine could be stopped for inspection of the specimen. After the machine was started again the next stringer and panel failed before the machine could be stopped. In some cases the motor was stopped before it had accelerated to normal speed in order to control the amount of cracking that took place between inspections. With this technique it was learned that a crack might pass through a stringer and a panel in less than 100 cycles of load with cracks frequently jumping as much as 1/2 inch per cycle after two stiffeners had failed.

As in tests of other configurations, the cracks grew more rapidly in 7075-T6 specimens than in 2024-T3 specimens. The crack-propagation curve for specimen 4B-1 does not appear in figure 10 because of the difficulties encountered in this test as described previously.

Stress Distribution

The results of strain-gage surveys made during representative tests are presented in figures 12 to 15. The sketch above each figure shows the extent of the crack at the time at which the indicated stresses were measured. The solid curves in each of these figures show theoretical stresses, corrected for shear lag (ref. 5), which apply at the critical section without a stress-raiser and without a crack. The points in parts (a) of these figures show the stress distributions present in each of the beams at the start of the tests to be in reasonable agreement with the theoretical stresses. The maximum variation in stress level across the width was approximately 3 ksi. (See data for beam 3B-1, fig. 14(a).) As might be expected, the stress at a given point in the skin increased as the crack approached that point. When the crack passed a given chordwise (across the width) station, the stress indicated by gages at that chordwise station decreased and finally approached zero. Obviously, those gages would have indicated zero stress if they had been immediately adjacent to the crack. For specimens on which the gages were applied at the critical section, the crack caused gage failure and no stress indication was obtained.

Stringer stresses also increased as the crack approached the stringer. In specimens made according to design 1, the stresses in a given stringer became very high when the crack had progressed one panel past that stringer (fig. 12(c)). In several cases the strain indication was out of the range of the measuring apparatus, or well into the plastic range. These high stresses account for the sudden failure of stiffeners in these beams. In specimens made according to design 2, the increase in stringer stress (fig. 13) was less, but still appreciable. The presence of rivet holes in these stringers undoubtedly contributed to stringer failure in designs 1 and 2.

A comparison between stress distributions in specimens 2B-2 and 3B-1 (see figs. 13(b) and 14(b)) indicates that, as the crack progressed through the first panel, the stress behavior in beams with riveted stringers was essentially the same as that in beams with bonded stringers. As the crack grew farther (figs. 13(c) and 14(c)), however, the stringers carried much less stress in bonded beams than in riveted ones. This fact, together with the absence of rivet holes in bonded stringers, explains why no stiffeners failed in specimens with bonded covers.

Figure 15 shows that, in integrally stiffened beams (design 4), the stresses in the skin and in adjacent stringers rose together. Since the skin and stiffeners were integral, the stiffeners did not slow down crack growth to any significant extent in this construction. At least one manufacturer using this type of construction (ref. 6) is using multiple units adjacent to each other to control the distance over which the crack can grow before a natural boundary intervenes.

Although the integral stiffeners offered little resistance to fatigue-crack propagation in this investigation, McBrearty (ref. 7) has shown a significant benefit of such stiffeners on static strength of panels containing cracks.

CONCLUSIONS

Fatigue tests of 18 box-beam specimens made of the two structural aluminum alloys, 2024-T3 and 7075-T6, and of four design configurations support the following tentative conclusions:

1. The number of cycles of load required to initiate a crack was approximately that which would be expected on the basis of tests of simple specimens. The scatter in results was also about normal for these materials. There was no significant difference between numbers of cycles of load required to initiate cracks in 2024-T3 aluminum alloy beams and those required to initiate cracks in 7075-T6 beams.

2. For a given configuration at a given stress level a fatigue crack grew more rapidly in 7075-T6 than in 2024-T3 aluminum alloy.

3. In specimens with riveted stringers the crack growth was interrupted each time the crack passed under a rivet head. Some cracks propagated without interruption along lines which bypassed rivets. A given stringer failed after the crack had grown at least one panel past that stringer.

4. In specimens with integral stiffeners, the crack grew steadily across the cover at the highest rate found in this investigation.

5. In specimens with bonded covers, the rate of crack propagation was influenced by the effectiveness of the bond. Cracks grew rapidly across the skin in specimens with poor bonds, but in specimens with good bonds the cracks grew at the lowest rate found in this investigation. No stiffeners failed in bonded specimens before the crack had grown completely through the skin. This result was probably attributable to the absence of stress-raisers in these stringers.

6. Strain-gage surveys indicated very large increases in stringer stresses just before stringer failure in specimens with four stringers. This stress increase was smaller in specimens with eight stringers riveted

to the cover and still smaller in bonded stringers. In integrally stiffened covers the stringer stress was essentially the same as the stress in the skin.

Langley Aeronautical Laboratory,
National Advisory Committee for Aeronautics,
Langley Field, Va., August 8, 1956.

REFERENCES

1. Grover, H. J., Hyler, W. S., Kuhn, Paul, Landers, Charles B., and Howell, F. M.: Axial-Load Fatigue Properties of 24S-T and 75S-T Aluminum Alloy As Determined in Several Laboratories. NACA Rep. 1190, 1954. (Supersedes NACA TN 2928.)

2. McGuigan, M. J., Jr., Bryan, D. F., and Whaley, R. E.: Fatigue Investigation of Full-Scale Transport-Airplane Wings - Summary of Constant-Amplitude Tests Through 1953. NACA TN 3190, 1954.

3. Neuber, Heinz: Theory of Notch Stresses: Principles for Exact Stress Calculation. J. W. Edwards (Ann Arbor, Mich.), 1946.

4. Kuhn, P.: Effect of Geometric Size on Notch Fatigue. Int. Union of Theor. and Appl. Mech. Colloquium on Fatigue (Stockholm, May 1955), Springer-Verlag (Berlin), 1956, pp. 131-140.

5. Kuhn, Paul: Stresses in Aircraft and Shell Structures. McGraw-Hill Book Co., Inc., 1956.

6. Stone, Irving: Electra Structure Reveals Refinements. Aviation Week, vol. 65, no. 1, July 2, 1956, pp. 58-60.

7. McBrearty, J. F.: Fatigue and Fail Safe Airframe Design. Preprint No. 610, paper presented at SAE Golden Anniversary Aeronautic Meeting, Los Angeles, Calif., Oct. 11-15, 1955, SAE, Inc. (New York 18, N. Y.).

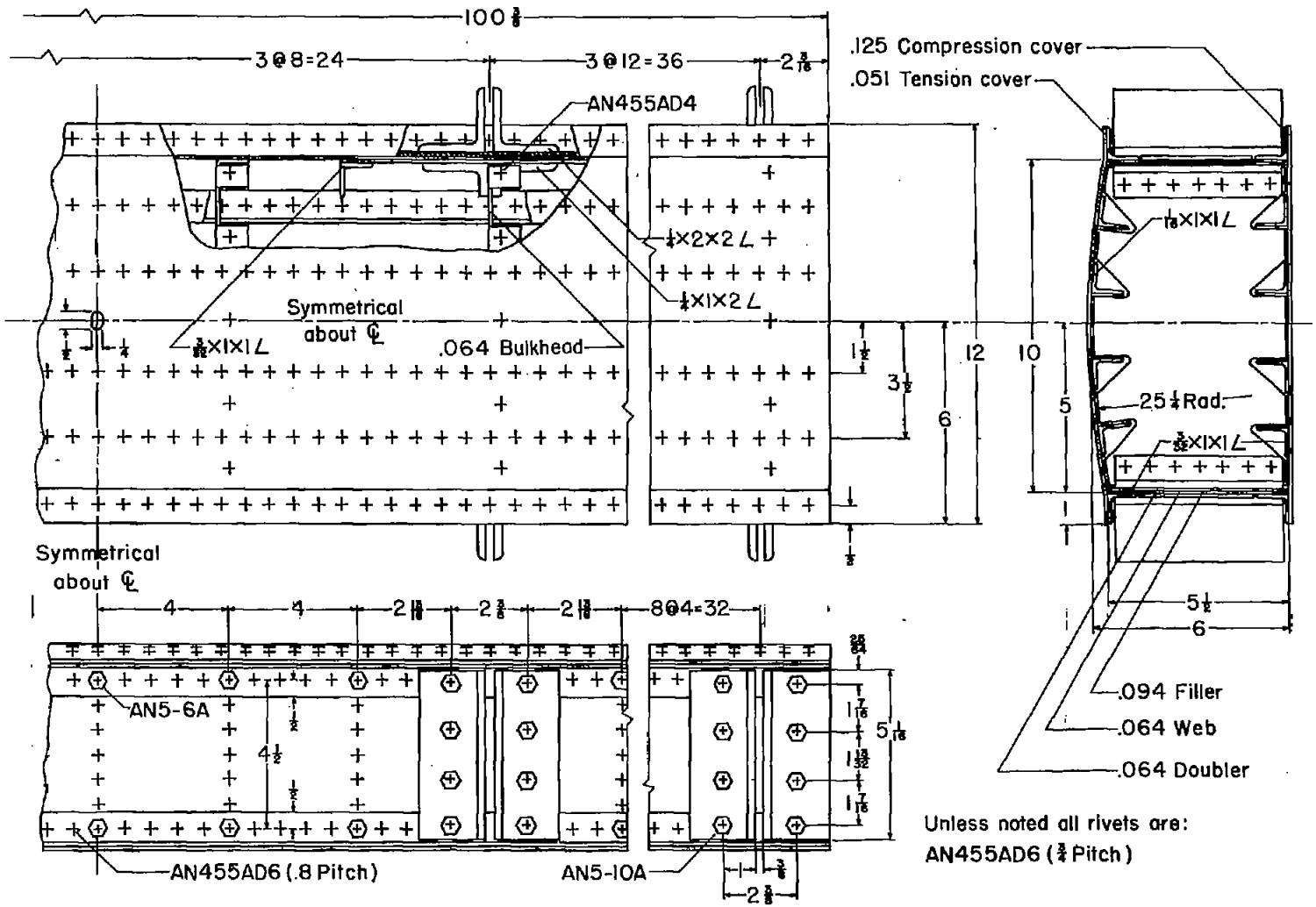

Figure 1.- Design 1. (All dimensions are in inches.)

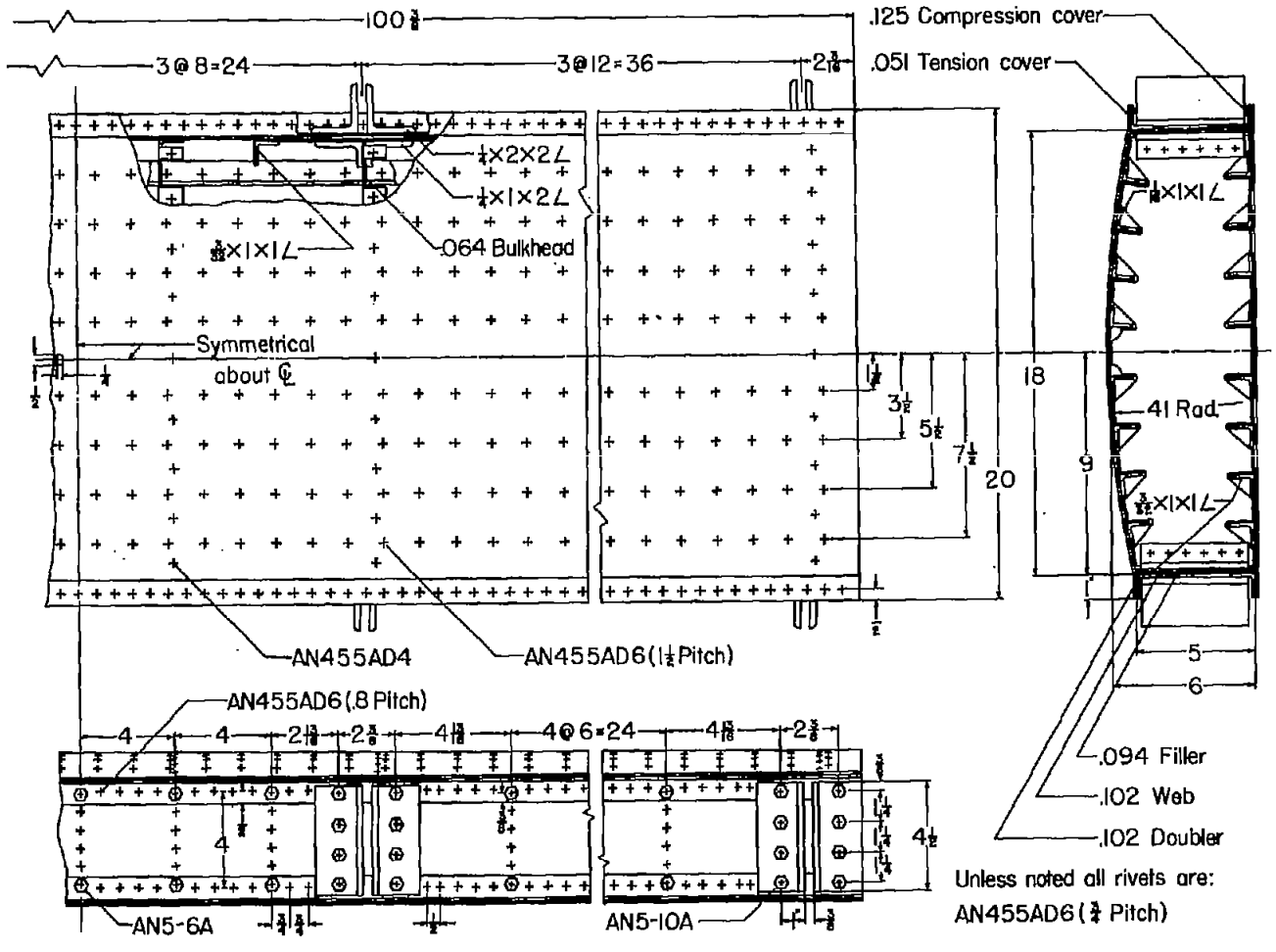

Figure 2.- Design 2. (All dimensions are in inches.)

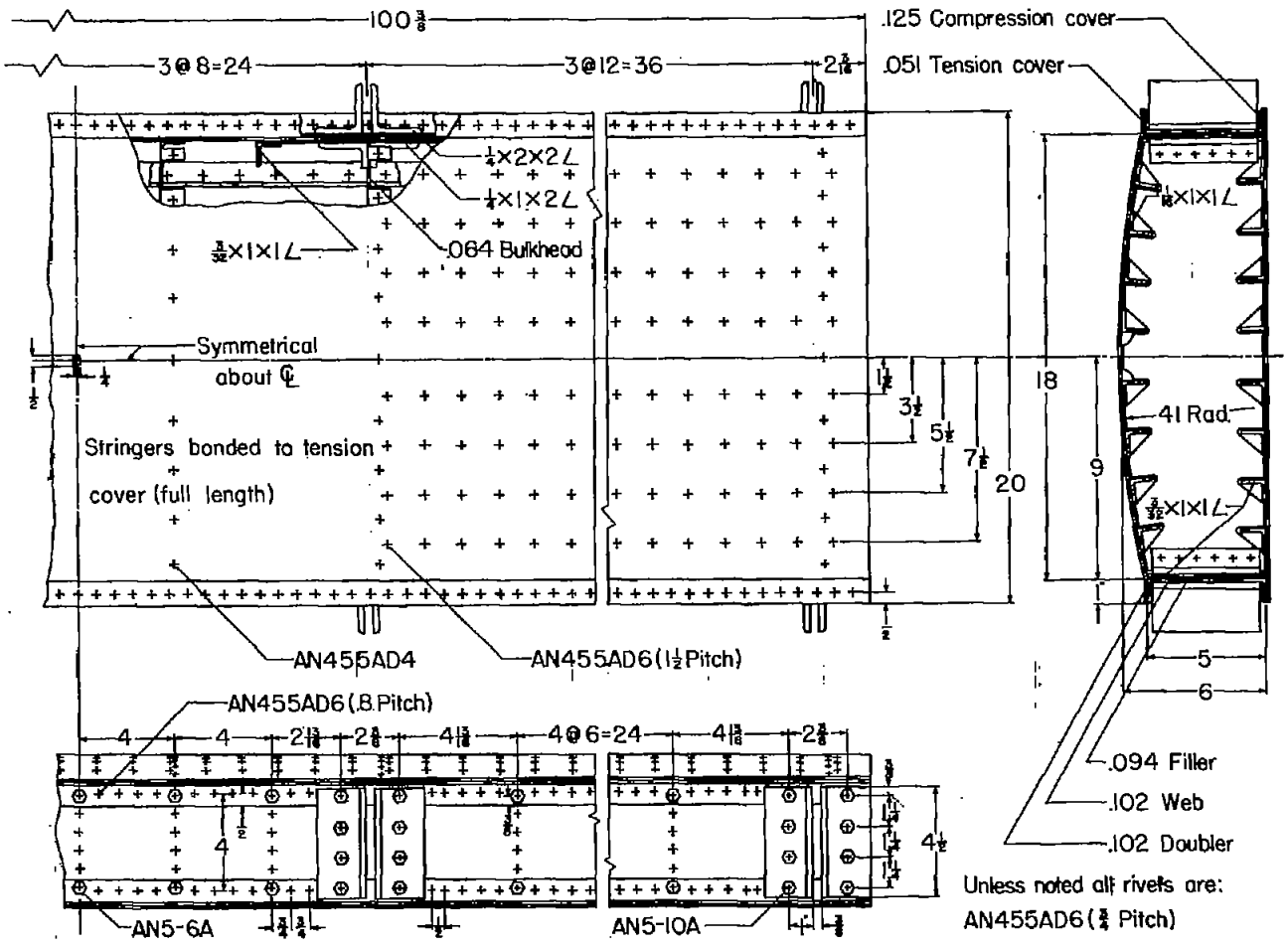

Figure 3.- Design 3. (All dimensions are in inches.)

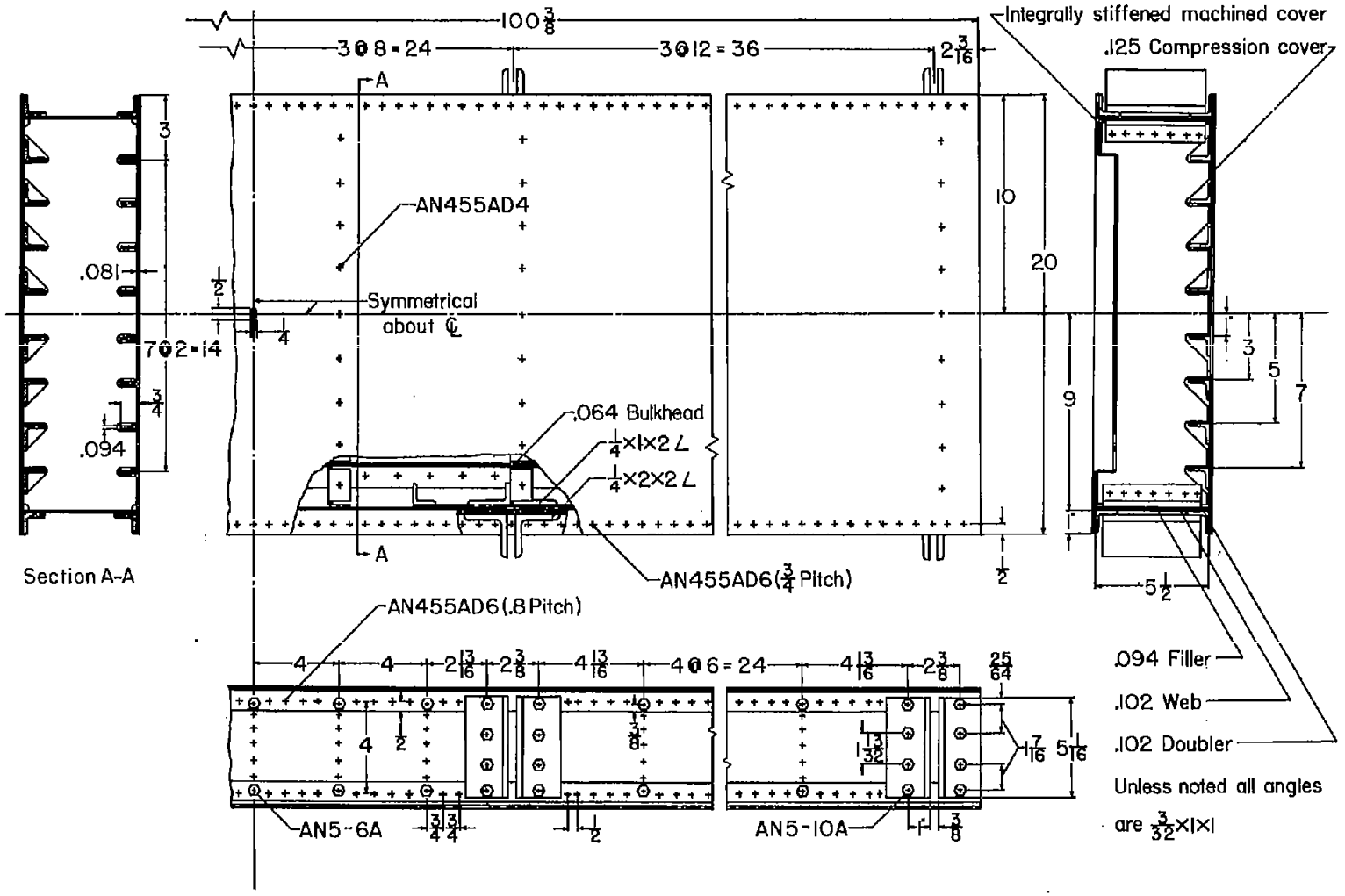

Figure 4.- Design 4. (All dimensions are in inches.)

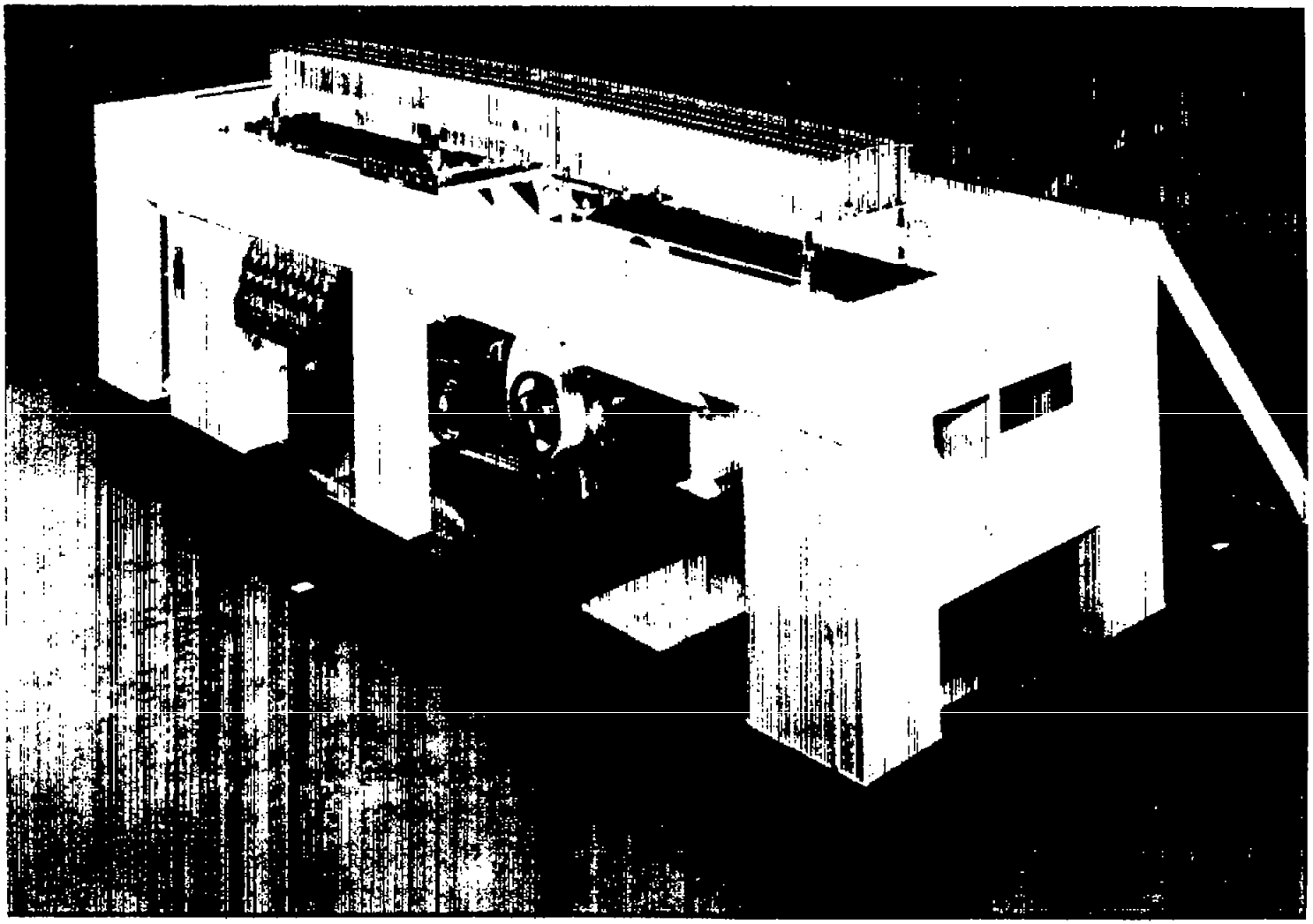

L-88554

Figure 5.- Box-beam fatigue-testing machine with specimen 1A-1 in place.

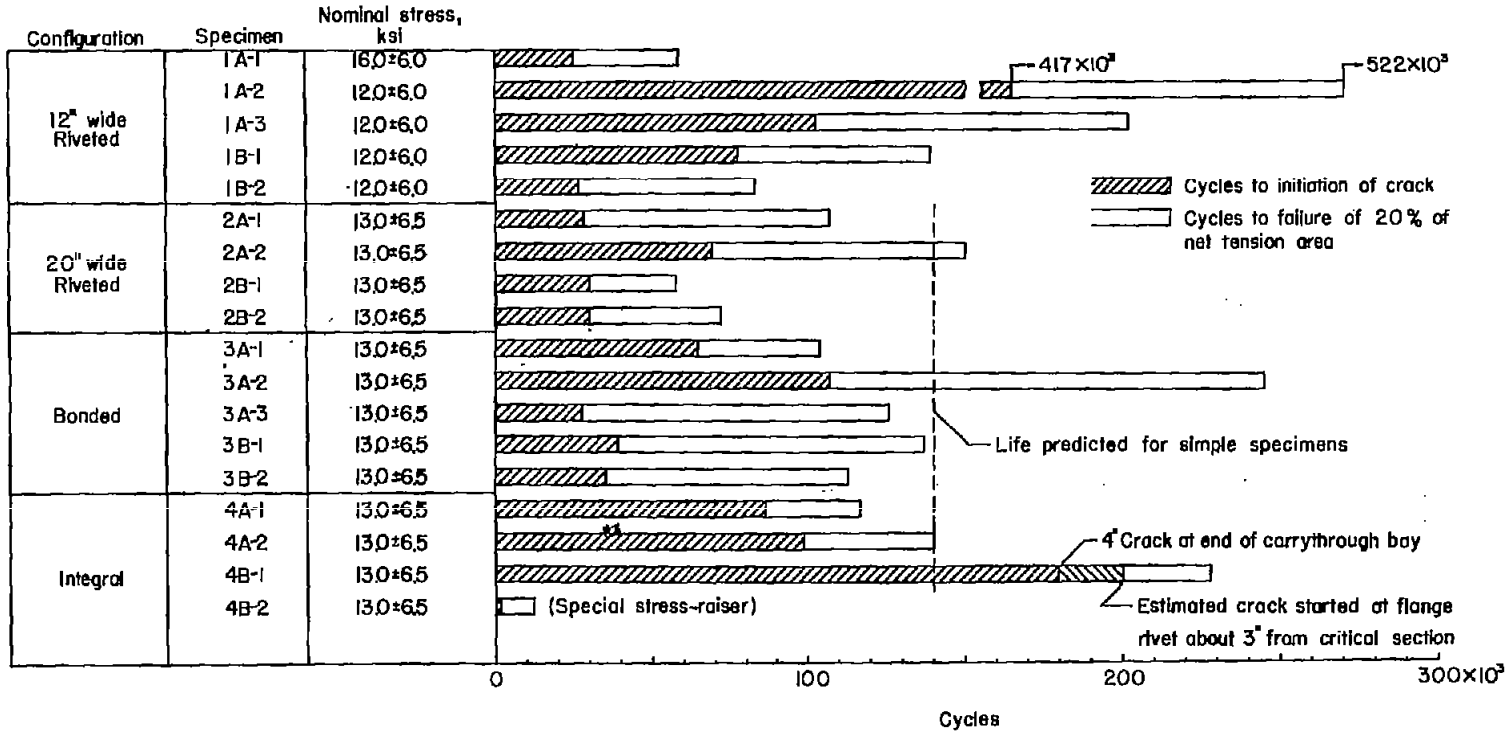

Figure 6.- Cycles required to initiate cracks in box beams. (Letters in specimen designation represent materials; A designates 2024-T3, B designates 7075-T6.)

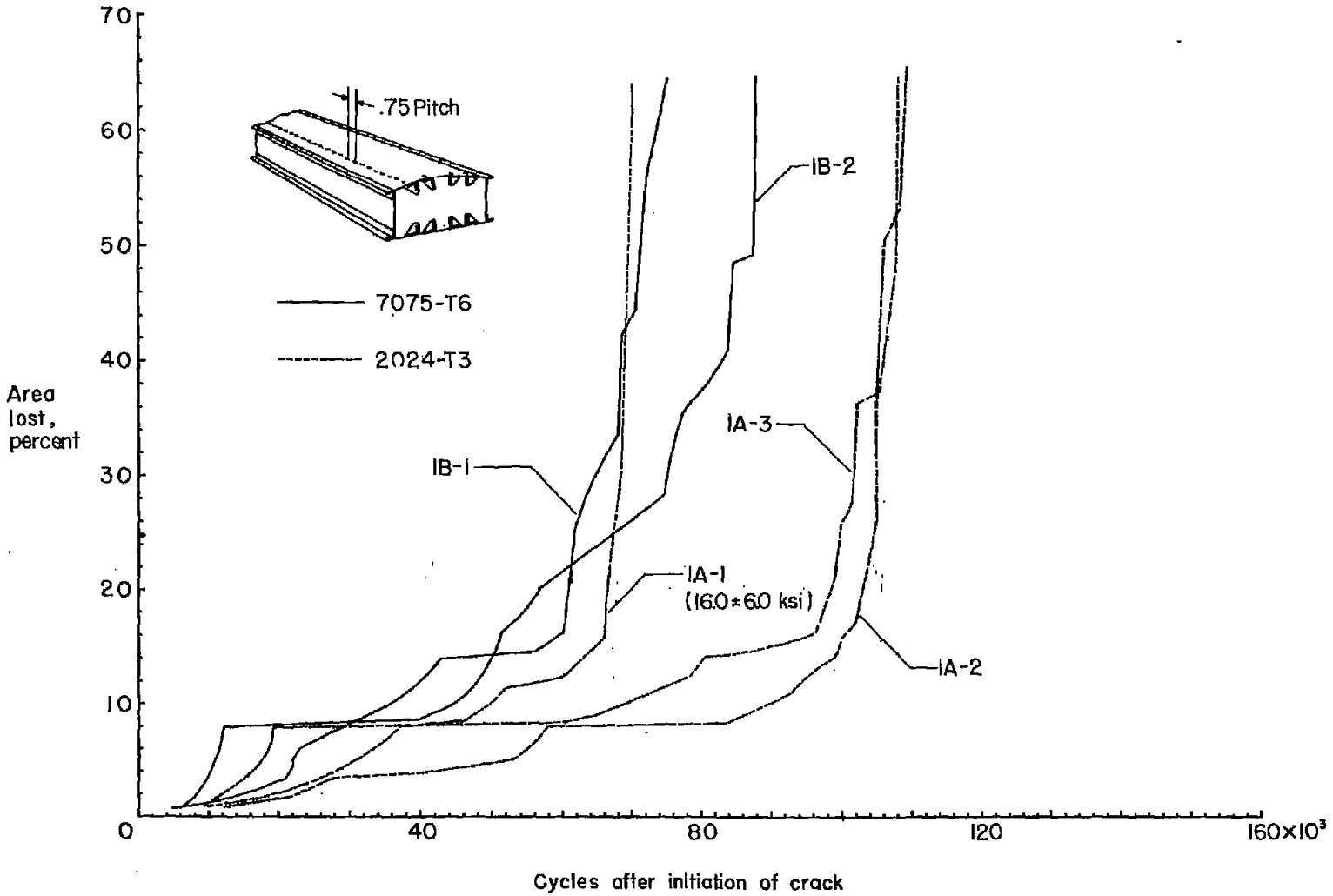

Figure 7.- Crack propagation in specimens of design 1 at maximum load. (Except as noted otherwise, stresses were 13 ± 6.5 ksi.)

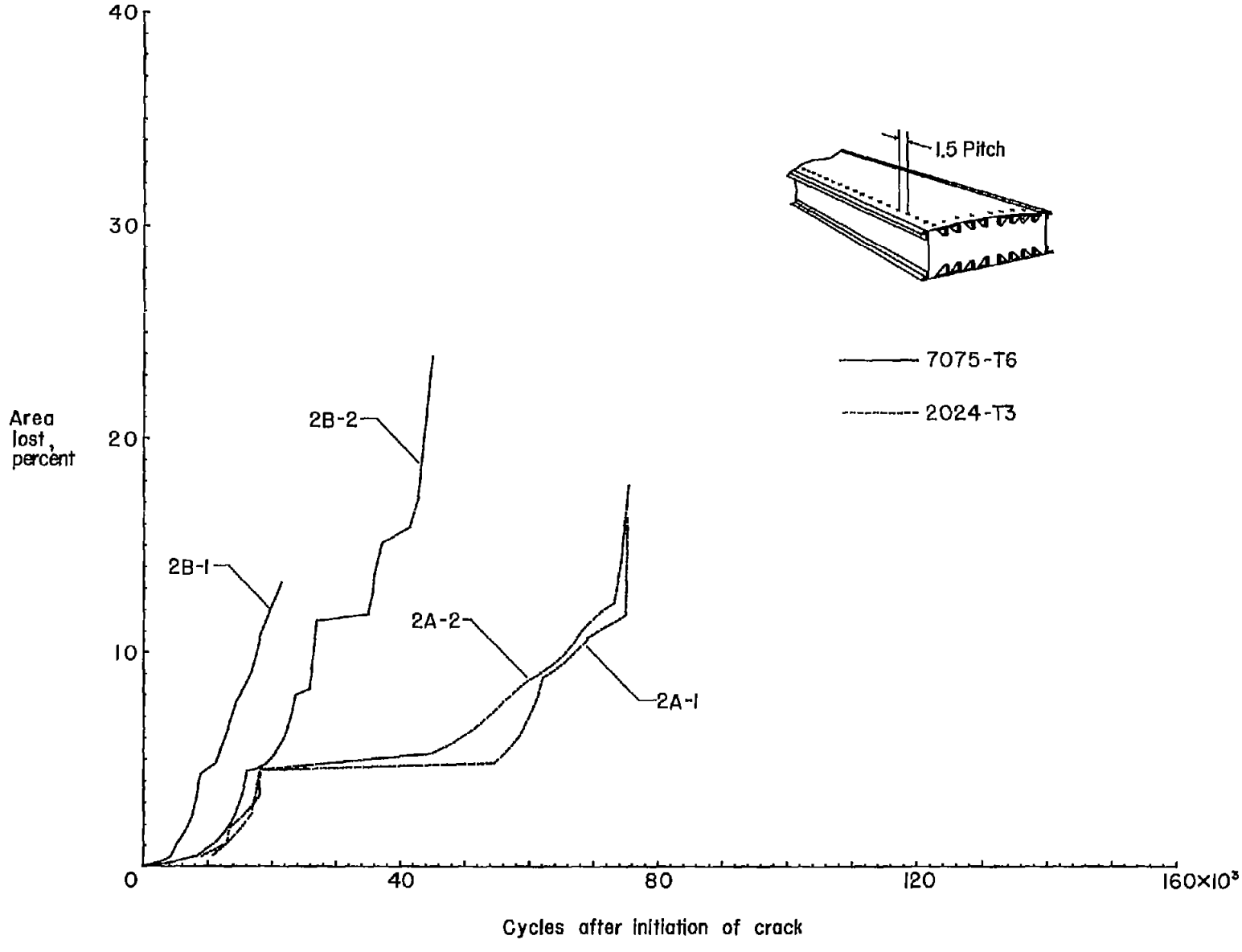

Figure 8.- Crack propagation in specimens of design 2. (Stresses were 13 ± 6.5 ksi.)

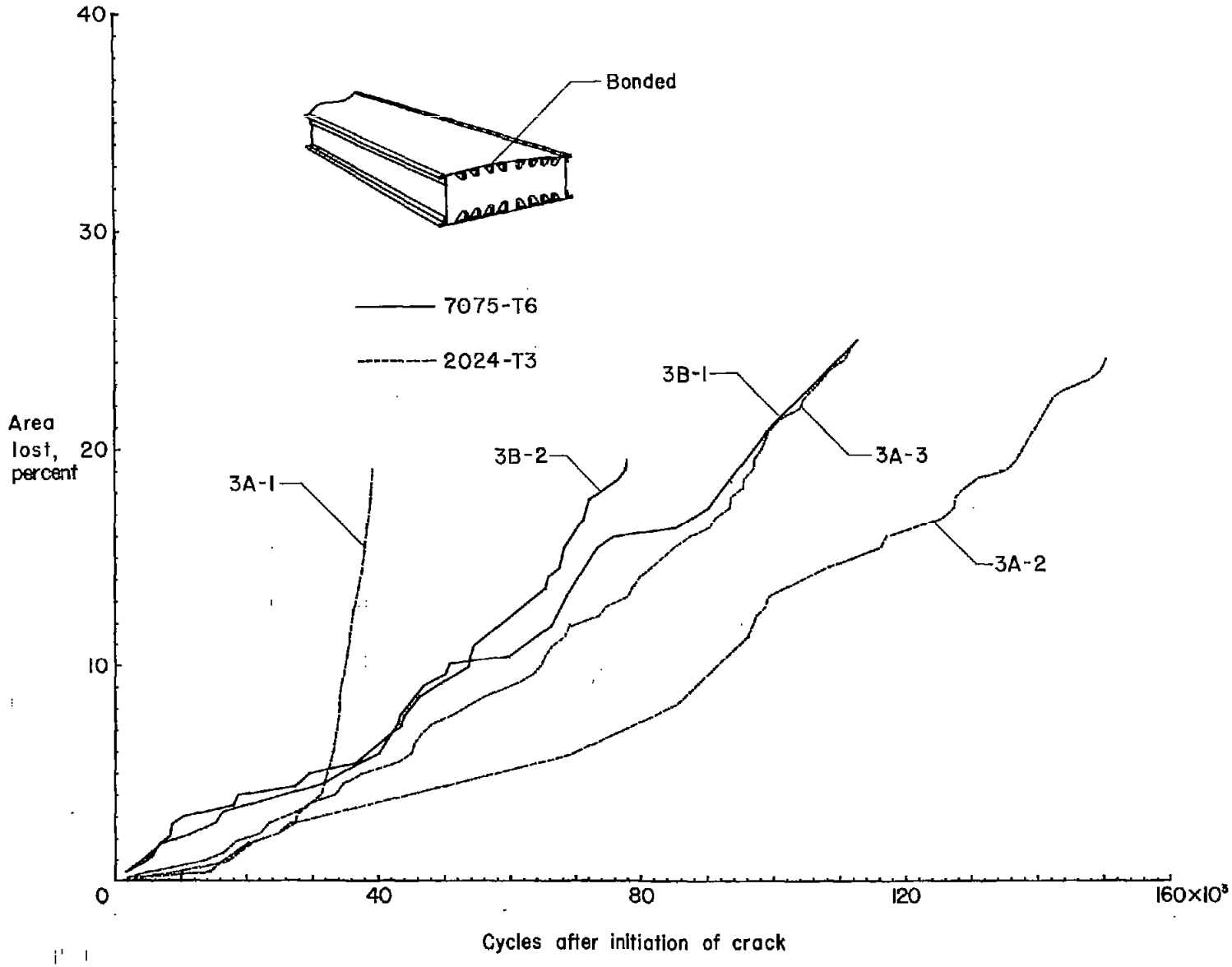

Figure 9.- Crack propagation in specimens of design 3. (Stresses were 13 ± 6.5 ksi.)

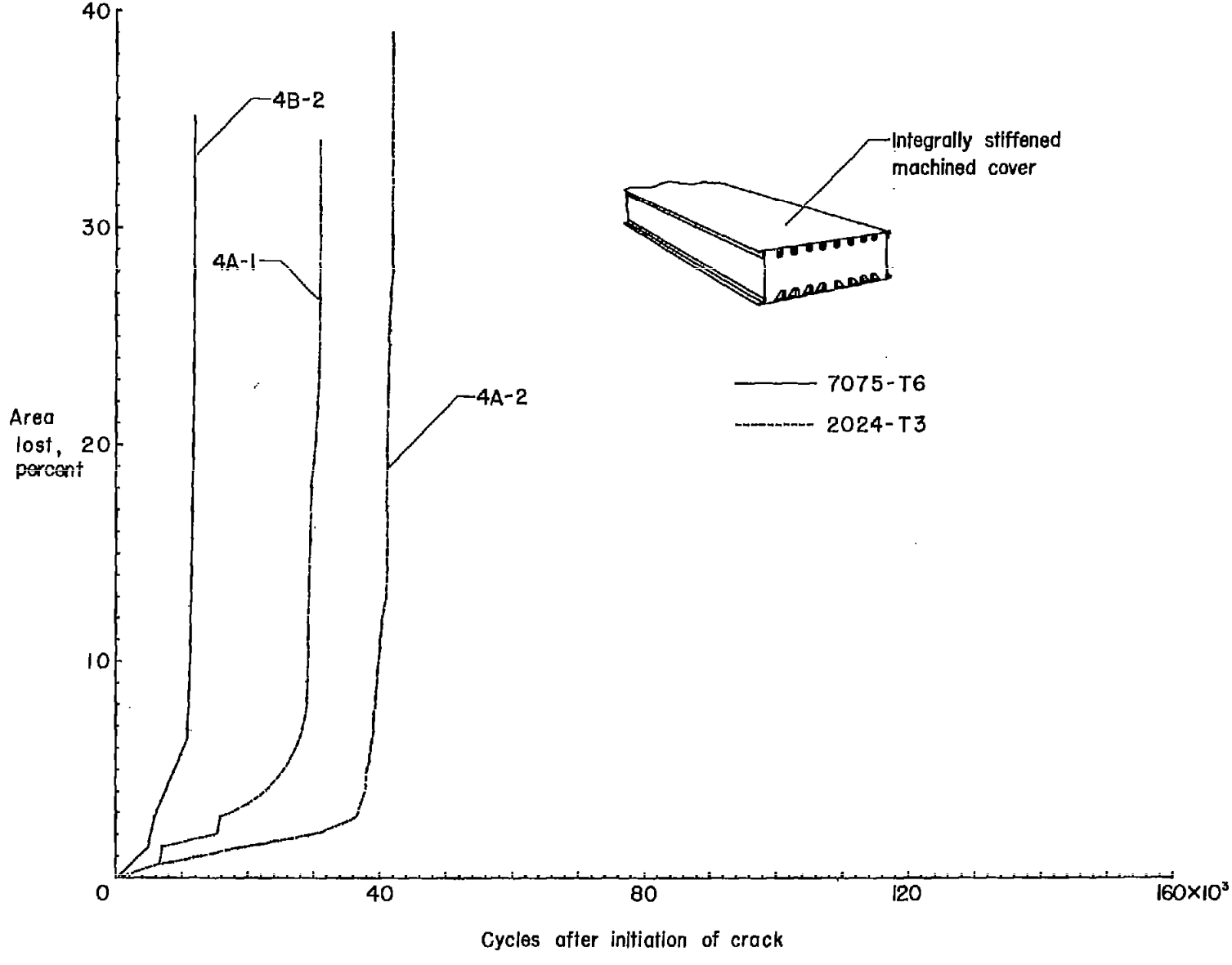

Figure 10.- Crack propagation in specimens of design 4. (Stresses were 13 ± 6.5 ksi.)

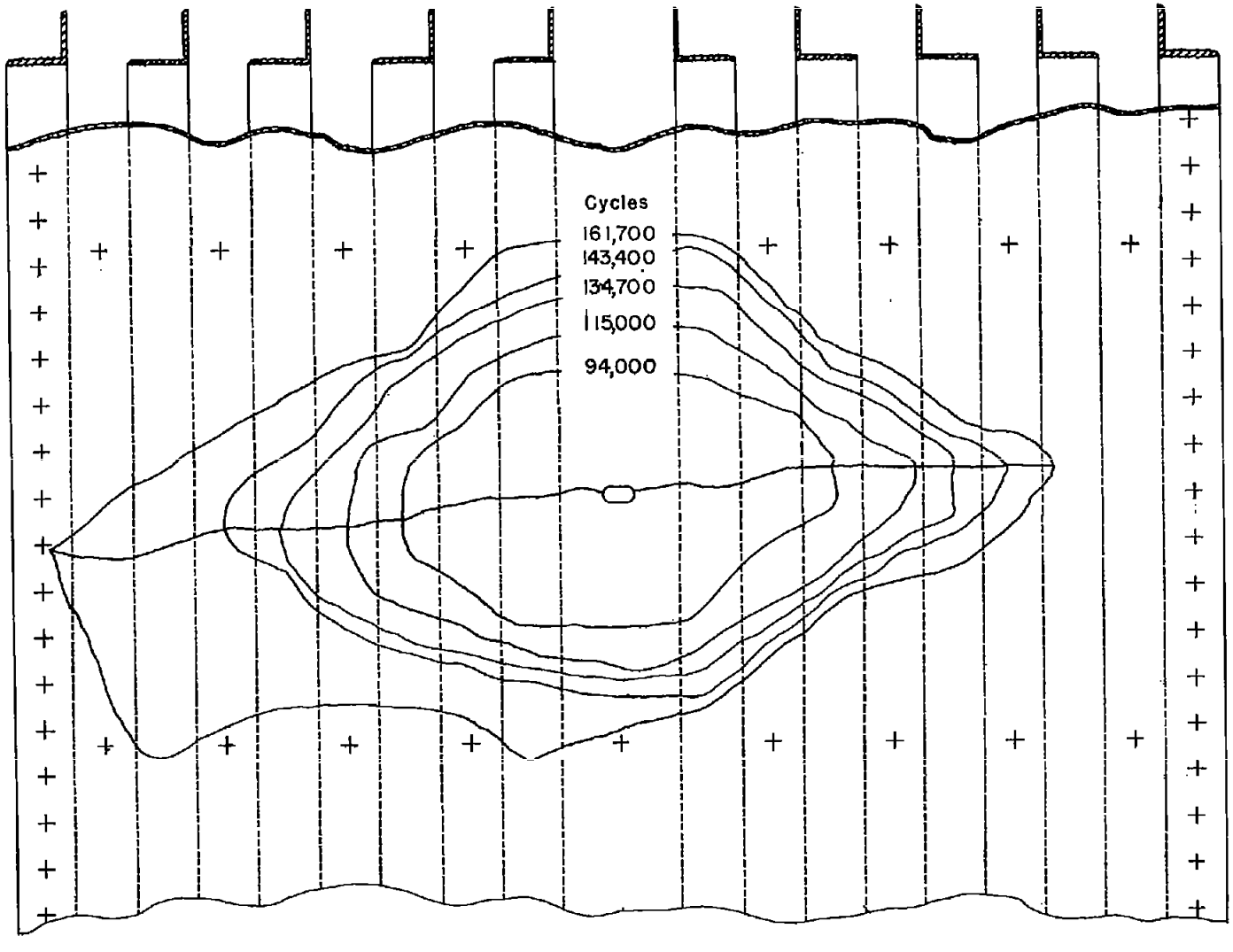

Figure 11.- Contours of bond separation in specimen 3B-1.

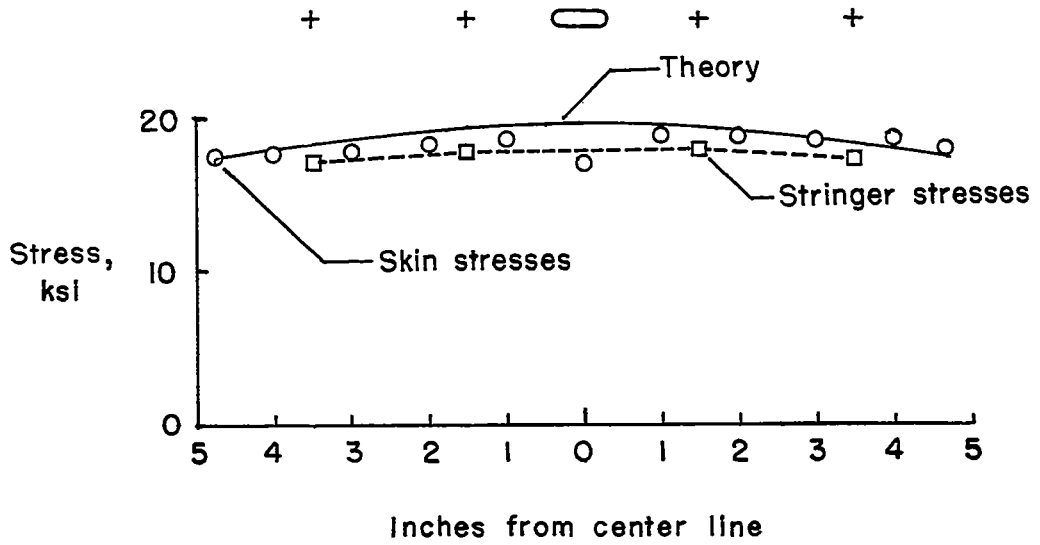

(a) At start of test.

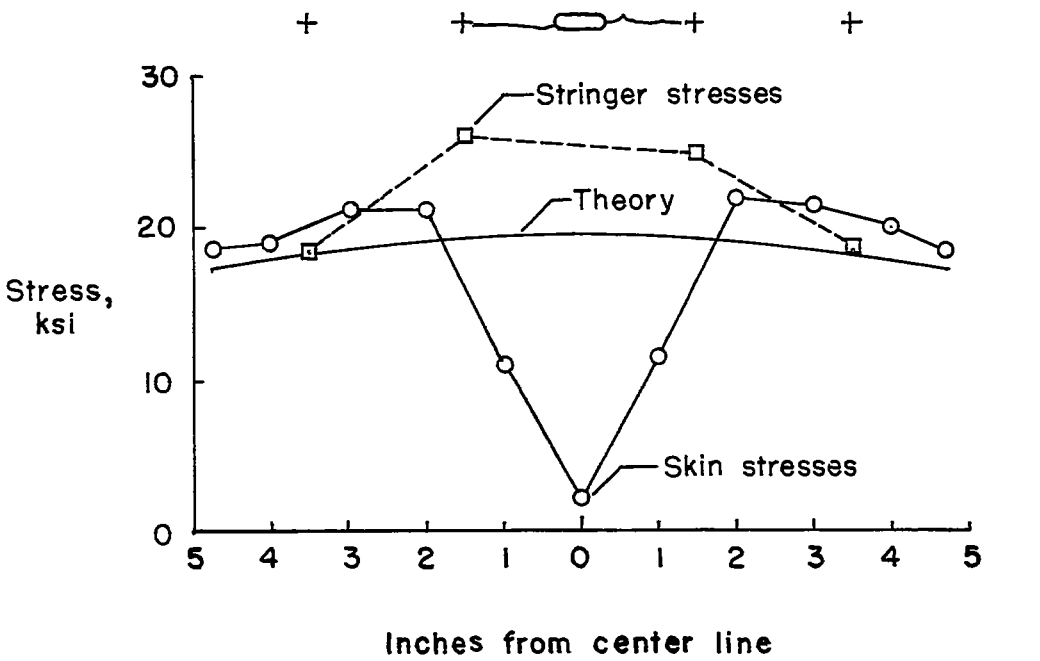

(b) 122,100 cycles.

Figure 12.- Stress distribution in specimen 1A-3 at maximum load. (Skin gages $1\frac{1}{2}$ inches from critical section.)

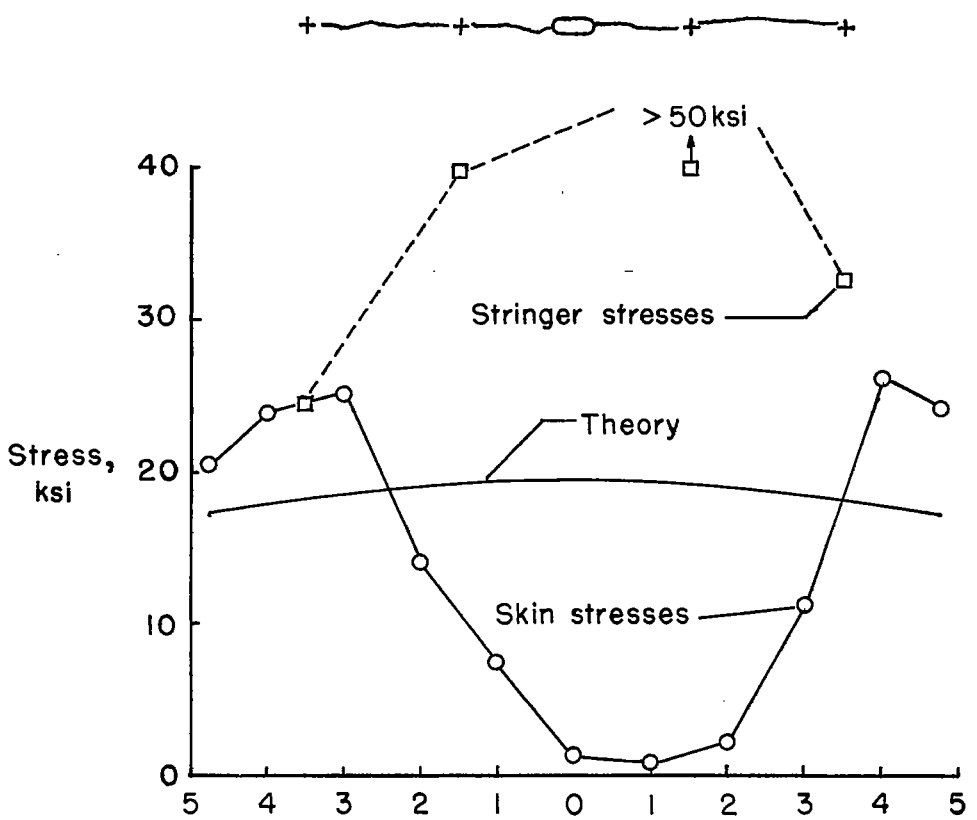

(c) 204,300 cycles.

Figure 12.- Concluded.

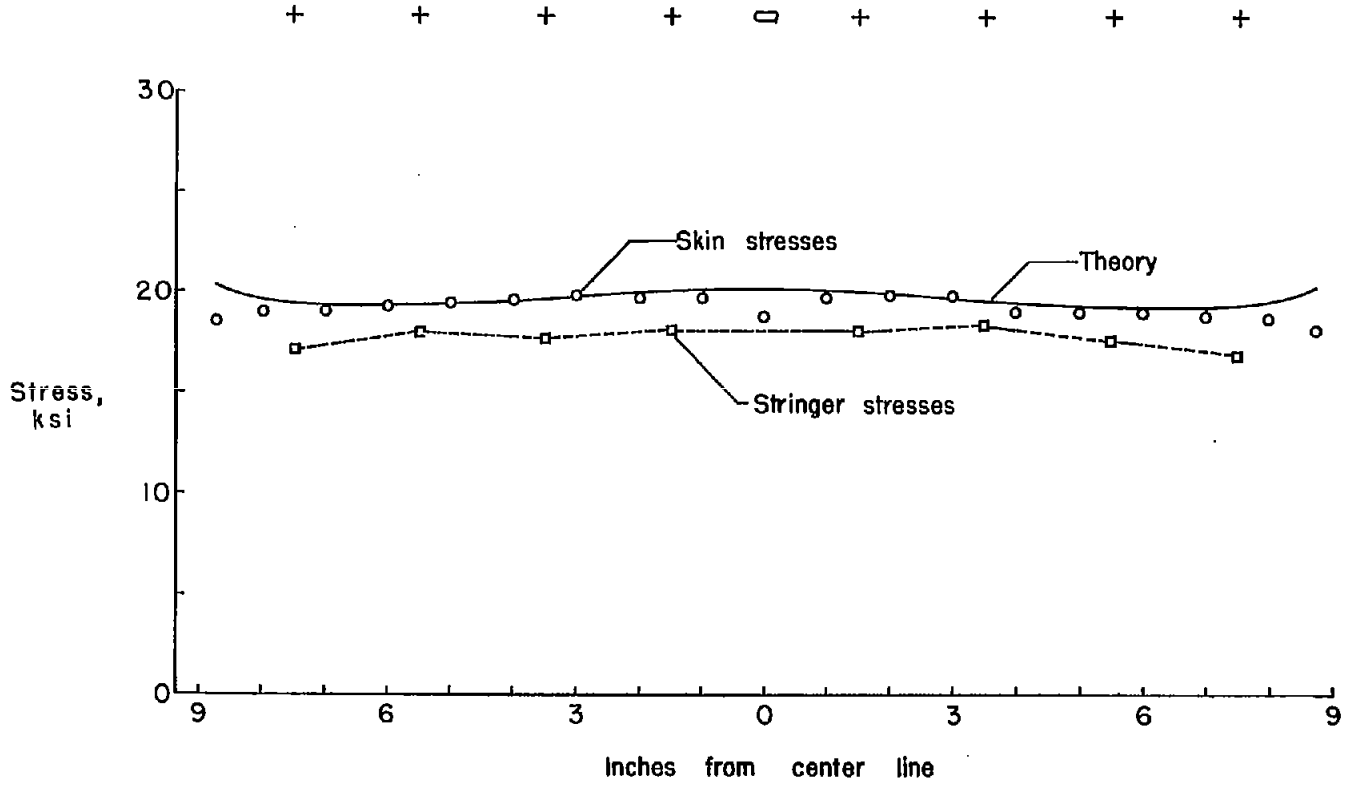

(a) At start of test.

Figure 13.- Stress distribution in specimen 2B-2 at maximum load. (Skin gages $1\frac{1}{2}$ inches from critical section.)

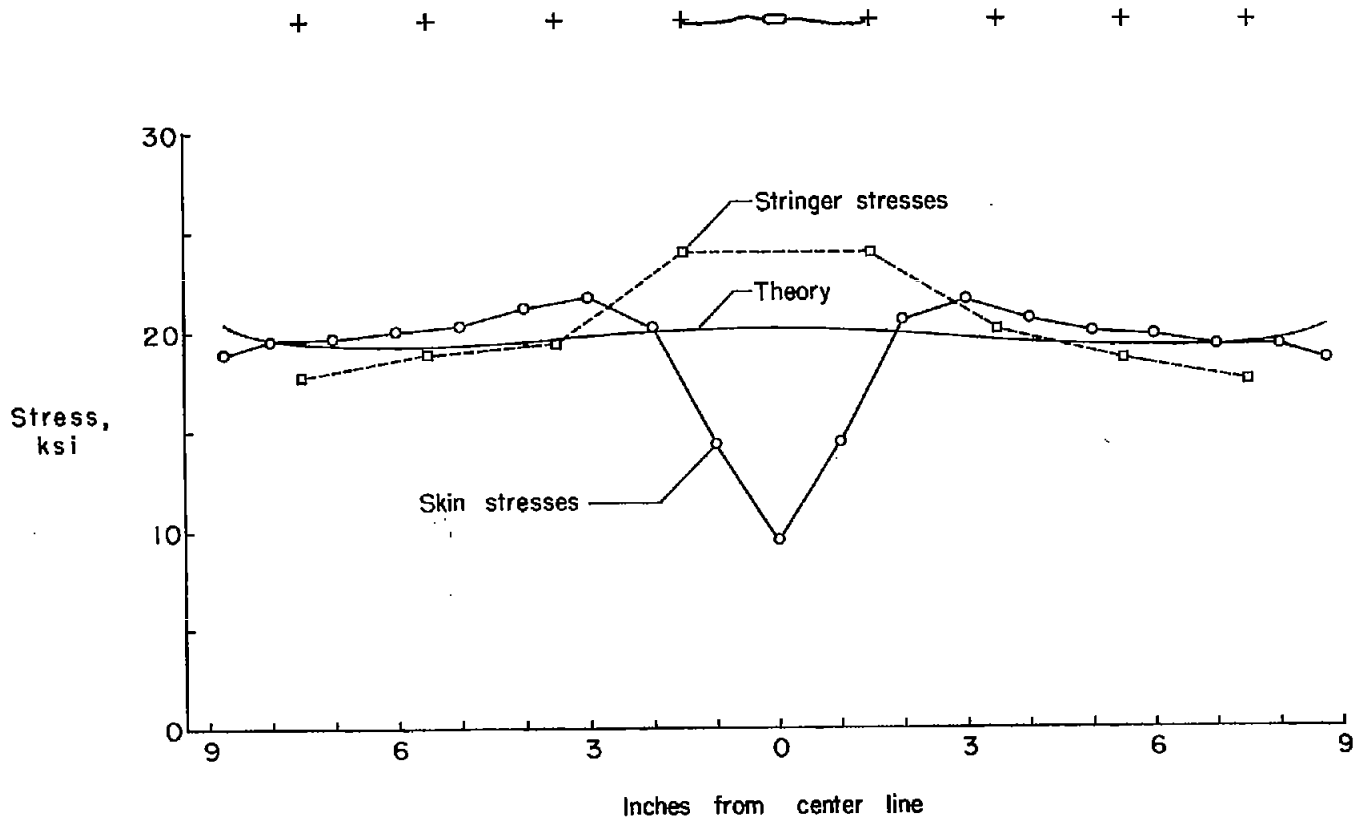

(b) 46,200 cycles.

Figure 13.- Continued.

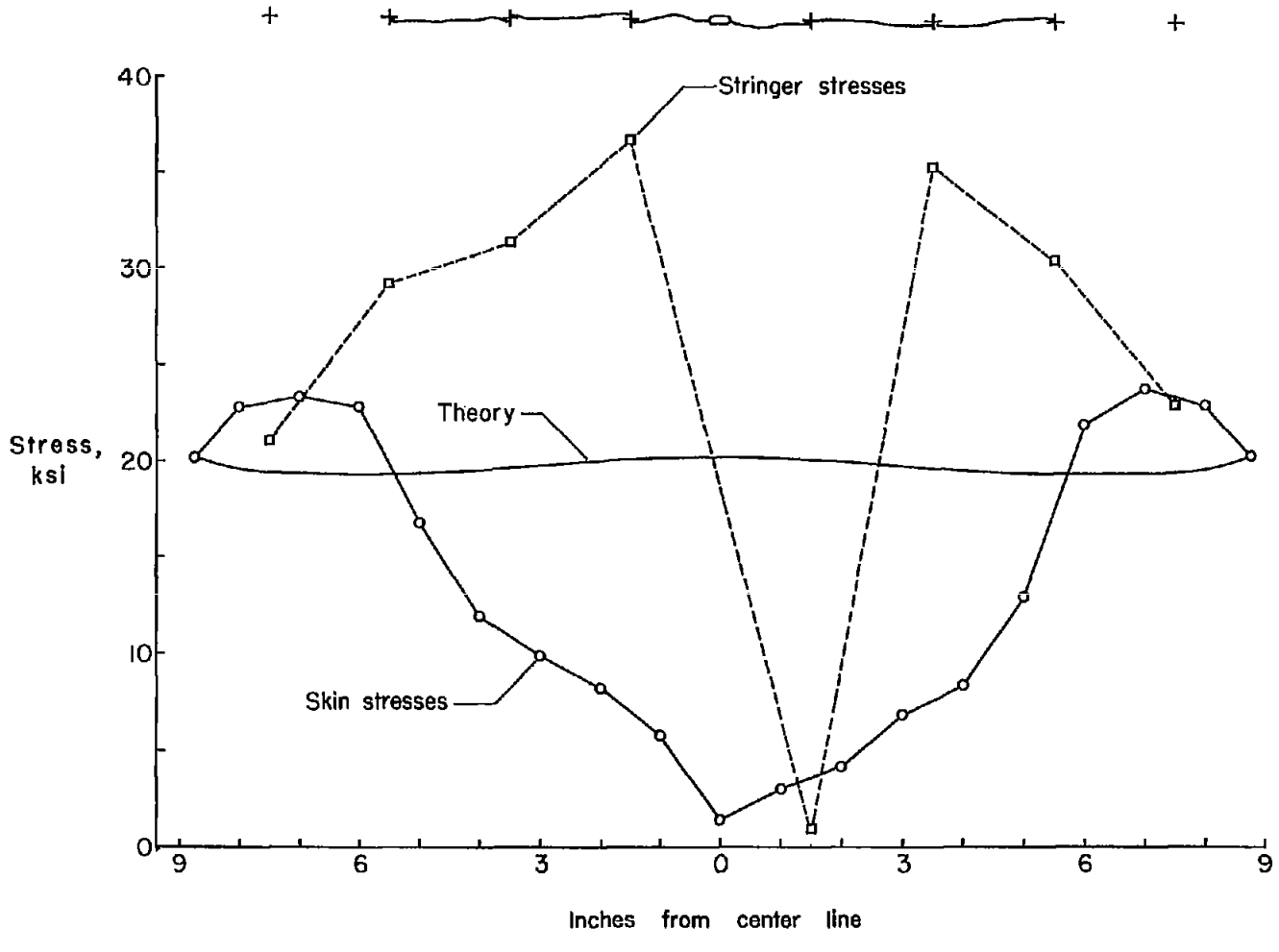

(c) 74,700 cycles.

Figure 13.- Concluded.

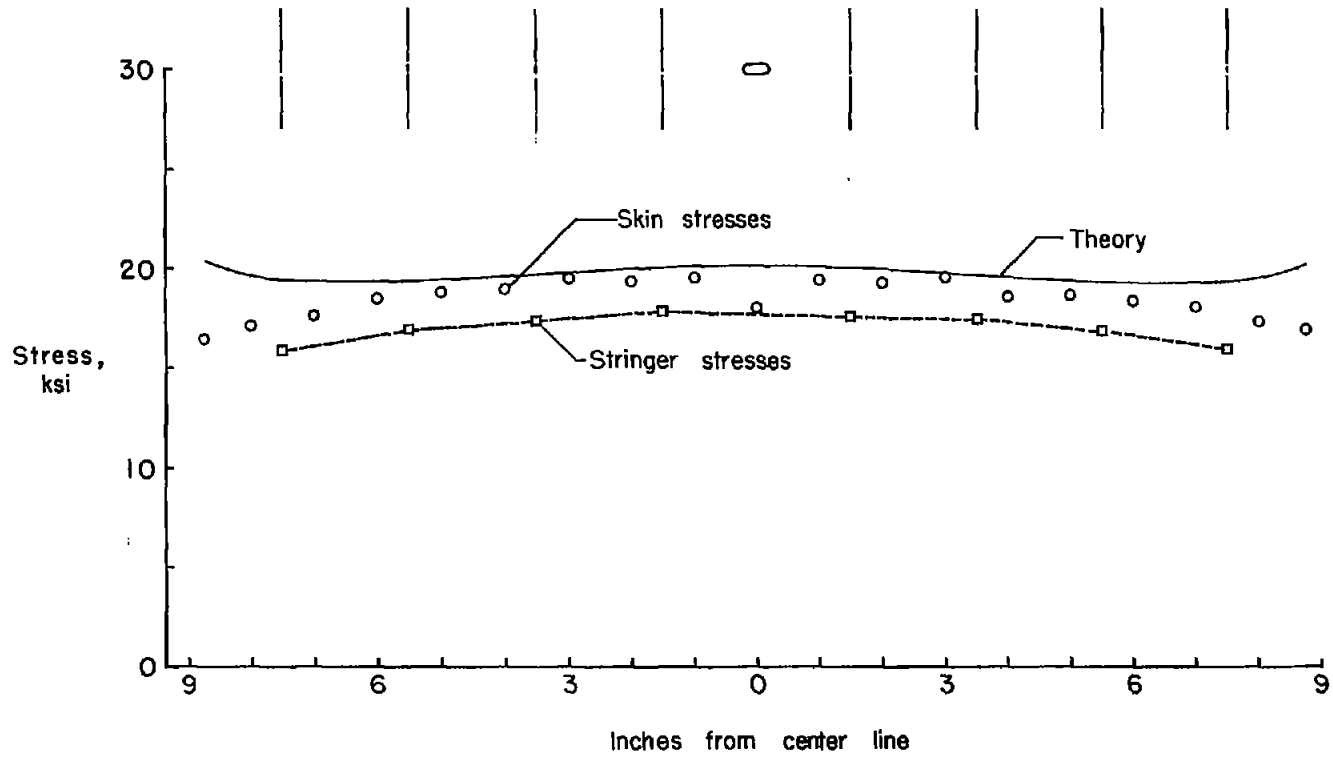

(a) At start of test.

Figure 14.- Stress distribution in specimen 3B-1 at maximum load. (Skin gages $1\frac{1}{2}$ inches from critical section.)

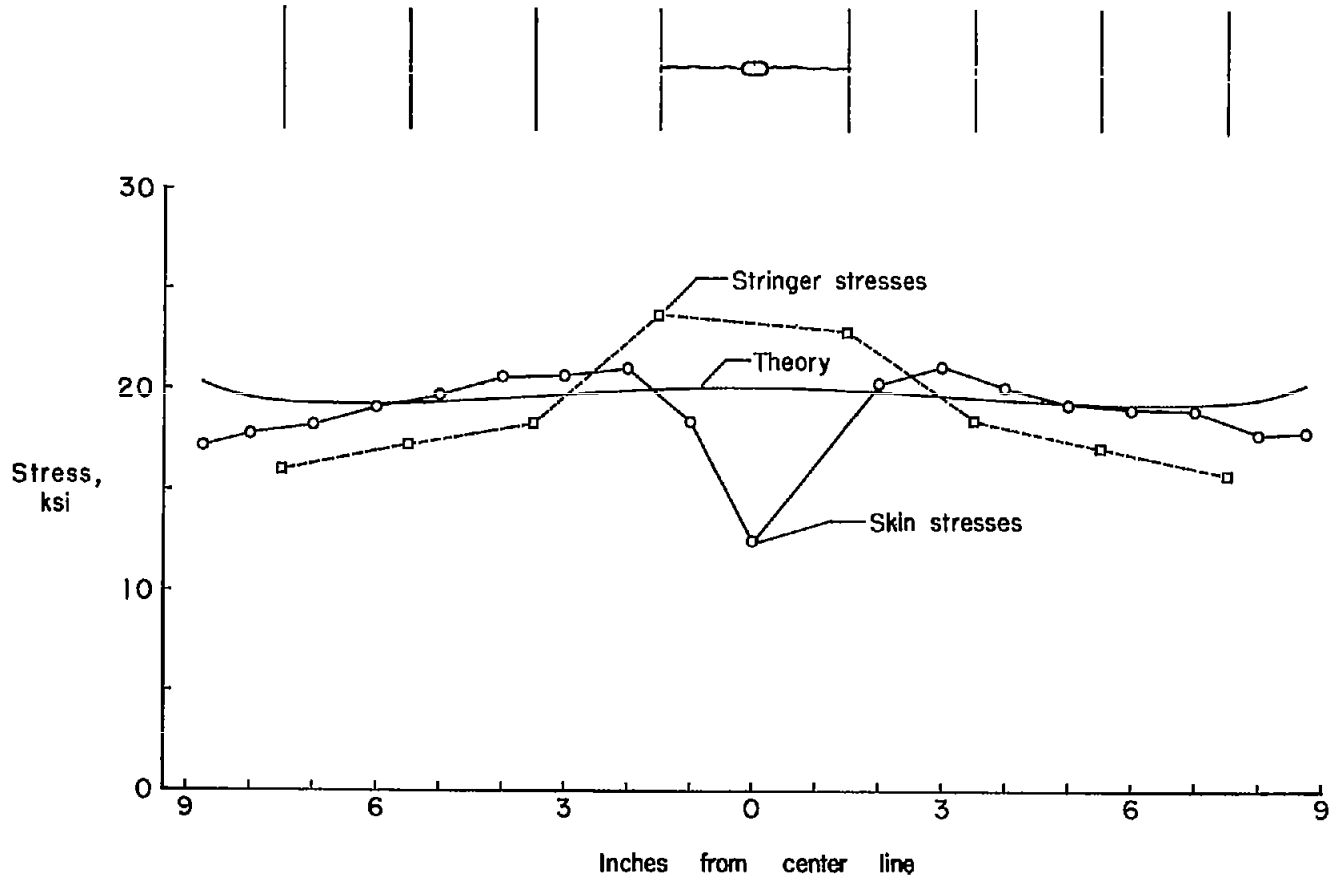

(b) 62,700 cycles.

Figure 14.- Continued.

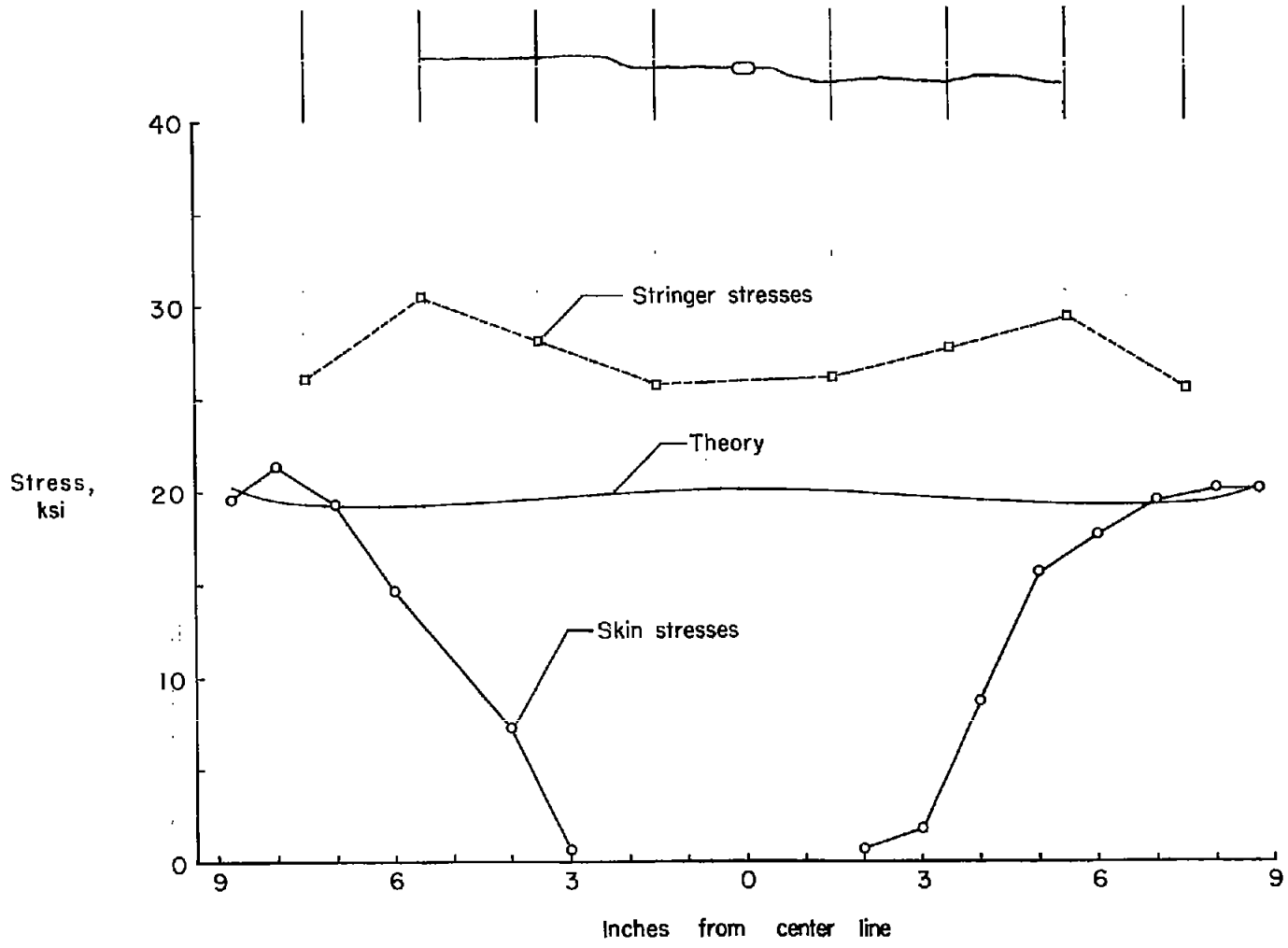

(c) 149,200 cycles.

Figure 14.- Concluded.

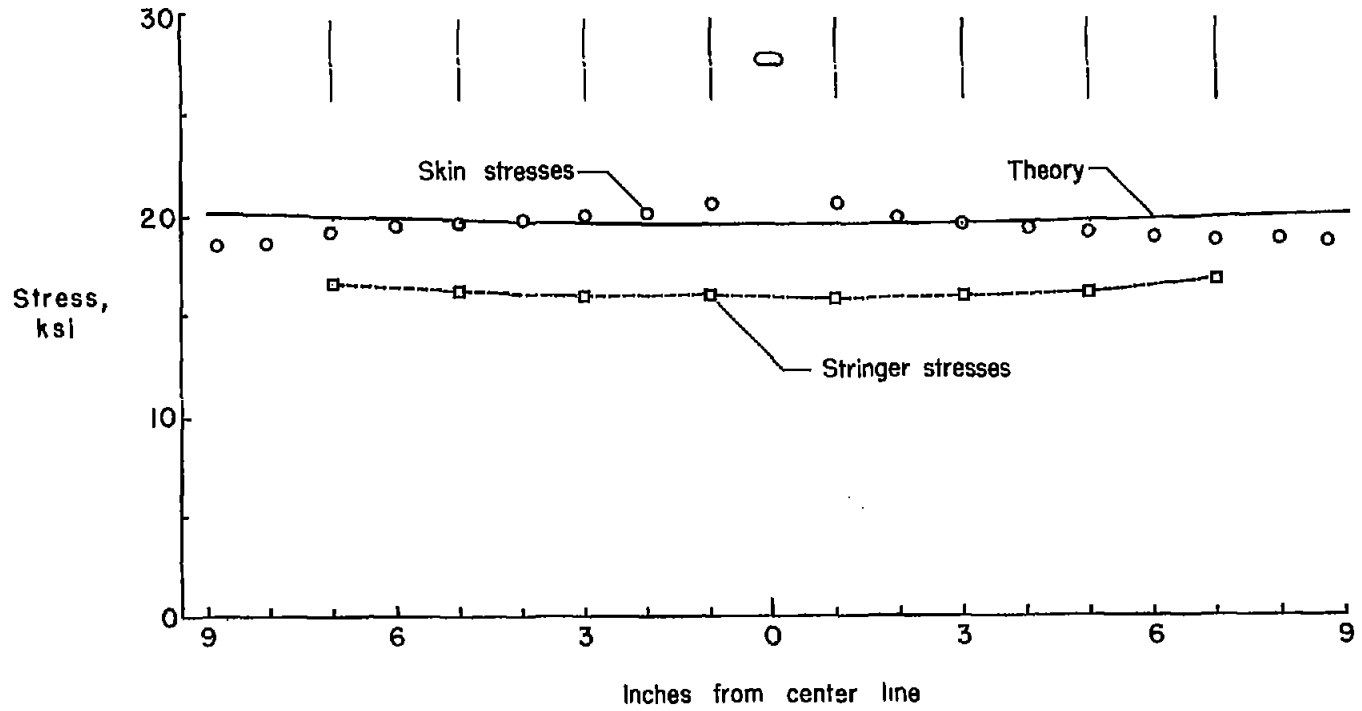

(a) At start of test.

Figure 15.- Stress distribution in specimen 4B-2. (Skin gages on critical section.)

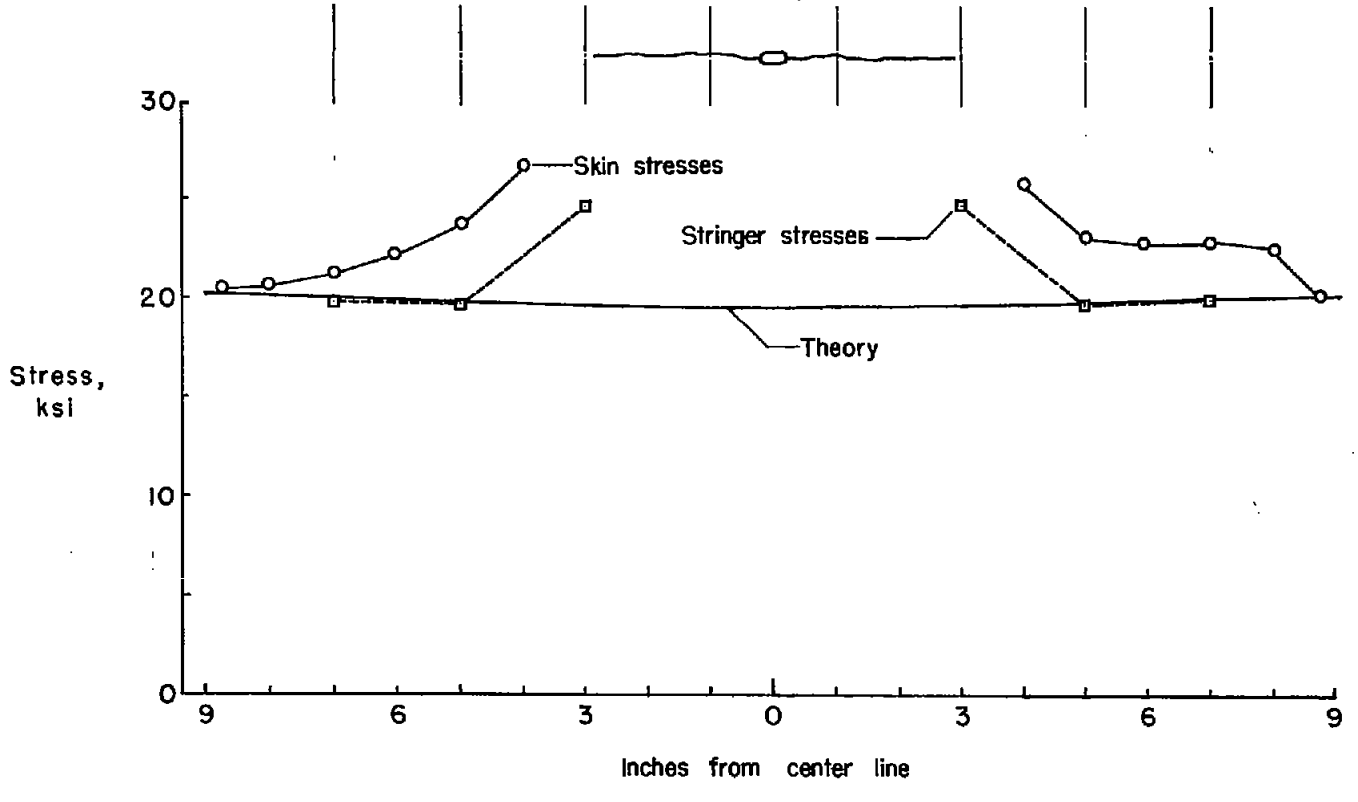

(b) 13,200 cycles.

Figure 15.- Continued.

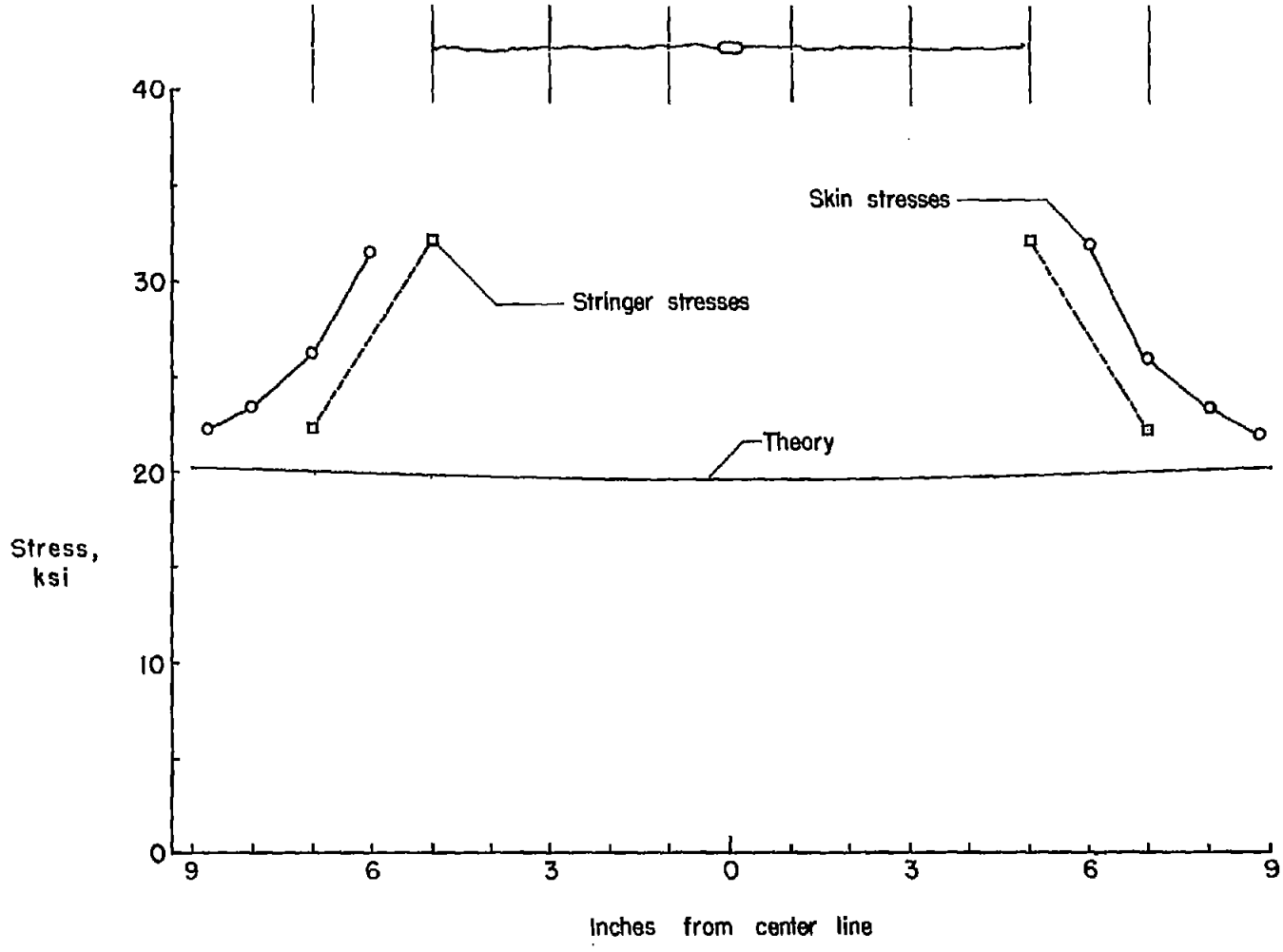

(c) 13,400 cycles.

Figure 15.- Concluded.